Materials Today Advances 14 (2022) 100227

Contents lists available at ScienceDirect

Materials Today Advances

journal homepage: www.journals.elsevier.com/materials-today-advances/

# A highly flexible form-stable silicone-octadecane PCM composite for heat harvesting

Xiang Yun Debbie Soo [a], Zhuang Mao Png [a], Ming Hui Chua [a], Jayven Chee Chuan Yeo [a], Pin Jin Ong [a], Suxi Wang [a], Xizu Wang [a], Ady Suwardi [a], Jing Cao [a], Yunjie Chen [a], Qingyu Yan [c, *], Xian Jun Loh [a, **], Jianwei Xu [a, b, ***], Qiang Zhu [a, ****]

[a] Institute of Materials Research and Engineering, Agency for Science, Technology and Research (A*STAR), 2 Fusionopolis Way, Innovis, #08-03, 138634, Singapore
[b] Department of Chemistry, National University of Singapore, 3 Science Drive 3, 117543, Singapore
[c] School of Materials Science and Engineering, Nanyang Technological University, 50 Nanyang Avenue, 639798, Singapore

ARTICLE INFO

*Article history:*
Received 29 November 2021
Received in revised form
21 February 2022
Accepted 21 February 2022
Available online 3 March 2022

*Keywords:*
Phase change materials
Flexible PCM
Form stable
Thermal management

ABSTRACT

Phase Change Materials (PCM) are efficient materials for thermal management and energy storage due to its high latent heat and recyclability. Many strategies have been employed to form stabilize PCMs through their phase transition; however these materials are almost invariably rigid. Herein a novel flexible form-stable PCM composite was successfully prepared by physical mixing and low temperature curing. They were well characterized in terms of various techniques including X-ray diffraction (XRD), Fourier transform infrared spectroscopy (FTIR), mechanical and leakage test, etc. A leakage test showed that the composite with 50% octadecane loading was form-stable with only 2.44% leakage. From the differential scanning calorimetry (DSC) results, the octadecane/silicone (Oct/Si) composite was found to possess a latent heat of 103.8 J/g, and an upshift in phase transition temperature was also observed from octadecane's melting point of 30.3 °C to between 34.4 and 37.8 °C, probably due to thermal insulation or microencapsulation by the silicone matrix. Thermogravimetric analysis (TGA) data supported its good thermal stability within this temperature range and mechanical testing of the composites further confirmed its flexibility and durability as evidenced by the Young's Modulus at 388.92 kPa and elongation at 341.42%, making Oct/Si composites useful for application in areas of temperature regulation, cooling, energy harvesting and wearable devices.



## 1. Introduction

Thermal energy management and storage is much sought after in many industry sectors such as construction, logistics, electronics etc., due to the escalating effects of global warming and increasing inclination towards sustainable energy sources. The most direct thermal management strategies includes using insulating materials such as aerogels [1], wools [2], foams [3] etc., in packaging, insulation boards and even concrete to reduce heat penetration; or to use infrared reflective coatings and paints [4–6] to reflect heat away. However, these technologies do not strive to make full use of the waste heat generated. More complex solutions such as thermoelectric materials [7–12] are able to tap on the waste heat at a thermal gradient to convert into useful electrical energy, but the efficiency in energy generation can still be improved significantly. PCM [13–17] on the other hand is able to absorb surrounding heat for cooling effect, and store the heat for later use such as heating up water tanks or prolonging a thermal gradient for thermoelectric devices etc, making it a favourable solution for thermal regulation.

There are three main classes of PCM; organic, inorganic and eutectic, and each has their own unique characteristics and disadvantages [18]. For near ambient conditions, organic PCMs such as paraffin wax, fatty esters, fatty acids and fatty alcohols are most commonly used due to their good thermal and chemical stability,

* Corresponding author.
** Corresponding author.
*** Corresponding author. Institute of Materials Research and Engineering, Agency for Science, Technology and Research (A*STAR), 2 Fusionopolis Way, Innovis, #08-03, 138634, Singapore.
**** Corresponding author.
*E-mail address:* zhuq@imre.a-star.edu.sg (Q. Zhu).

https://doi.org/10.1016/j.mtadv.2022.100227

low to no supercooling, high heat of fusion and generally non-corrosive nature with low toxicity [18]. To counter the leakage problem, researchers has come up with several solutions where macroencapsulation [19] is seen as the most direct and effective method where PCM was filled in a physical container and sealed. However, the bulky containment may not be suitable for applications requiring small amounts of PCM or have space constrains. Microencapsulation [20] or nanoencapsulation [21] on the other hand confine PCM in the core of a polymeric or inorganic shell. However, scale-up synthesis of these PCMs might be challenging and industries often look to spray drying methods for its production [22]. Form-stable PCM composites are a popular alternative, where it involves adsorbing PCM in porous inorganic materials such as expanded vermiculite [23], perlite [24], montmorillonite [25] and diatomite [26], and carbon materials such as expanded graphite [27], carbon nanotubes [28] and graphene aerogels [29] via capillary forces and interfacial tension within the pores [30,31] through vacuum impregnation. It also includes blending PCM with an organic polymer matrix such as high density polyethylene (HDPE) [32], polypropylene (PP) [33], low density polyethylene (LDPE) [34], linear low density polyethylene (LLDPE) [35] etc. via the melt method [36] or using an extruder [37]. Form-stable PCMs are thus able to prevent leakage and maintain the shape of the composite when held above its phase transition temperature [38].

Nevertheless, form-stable PCMs are generally stiff and rigid, and may not be applicable in areas that require some degree of flexibility such as wearable devices and thermal lagging that lines irregular shaped objects. In electronics, high rigidity may lead to high thermal contact resistance between the PCM composites and target devices, which may reduce the performance of the device [39]. Hence, flexible form-stable PCM composites would be useful for such purposes. Several flexible form-stable PCMs have been reported, where some of their works have been summarized in Table S1 [40–44]. These flexible form-stable PCM systems in general include either organic PCMs such as paraffin wax, octadecane and PEGs, or metal salt-based inorganic PCMs, with various polymers as matrixes, for example, block copolymer [40], polymer hydrogel [41,44] and silicone (this work). Wang et al. reported the flexible paraffin (PA)/olefin block copolymer composite [40] when the temperature is above $T_m$ of PA. However, this may render its applications slightly inconvenient, as heat has to be applied before the block copolymer is flexible for shaping. On the other hand, the PEG composite reported by Yuan et al. [41] deforms only under a specific temperature range when force is applied, which is useful for applications that require fixed shape components. However, care must be taken to shield it from external forces so as not to lose its shape, which poses an additional consideration during process. Lu et al. [42] prepared ethylene propylene diene monomer (EPDM)/PA shape-memory PCM, but requires a multi-step fabrication involving extruder and high temperature vulcanization. Liu et al. [43] and Jiang et al. [44] both prepared a stretchable yet durable form-stable PCM that is easier to use for irregular shaped components. In comparison, the use of inorganic based PCM may not be ideal as they suffer from supercooling, poor thermal cyclability and melting incongruency [45]. In this work, we fabricated a silicone-based flexible organic form-stable PCM which was prepared by physically mixing octadecane with silicone, and then curing at low temperature. They are versatile in applying for irregular shaped objects. Studies showed that they exhibited good thermal stability with flexibility and durability as evidenced by the measurement of Young's Modulus and elongation, making them useful for applications in areas of temperature regulation, cooling, energy harvesting and wearable devices.

Octadecane is a long chain hydrocarbon with a high latent heat of approximately 244 J/g and a melting point of about 28 °C [46]. With its working range close to ambient temperature, octadecane is commonly used as a PCM for heat regulation or energy storage in buildings [47], batteries [48], fabrics [49] and many other areas. Silicone is known for its durability and flexibility, and is highly chemical resistant, non-flammable and a good insulator. It has been extensively researched in areas such as stretchable wearable electronics [50,51] and biomedical applications [52]. As far as we know, no research was done for incorporating PCM into silicone to harness its flexible properties for thermal management. Most research involved silicone as a shell material for microencapsulated PCM [53]; as a form-stable PCM matrix to blend with microencapsulated PCM [54]; or a stiff form-stabilised PCM-silicone composite [55]. With flexible electronics and wearables gaining importance for real time monitoring of human health, and the ever-persistent issue of global warming, there is a need for a flexible energy harvesting or thermal regulating component to complement the existing technologies.

Herein, we successfully incorporated octadecane into silicone to generate a highly flexible form-stable PCM. Composites with different octadecane loading in silicone matrix were prepared and evaluated for its leakage, form-stability, thermal properties, and phase change properties at different Oct/Si mass ratios. The as-prepared Oct/Si composites exhibit great flexibility with moderately high latent heat storage capacity, making them a useful material for thermal energy storage applications.

## 2. Experimental section

### 2.1. Materials

Silicone rubber cured by a two-part system, PlatSil® 73-20 Part A and PlatSil® 73-20 Part B, at room temperature was purchased from Polytek Development Corp. *n*-Octadecane with chemical purity 98% was purchased from by Beyond Industries (China) Limited. All chemicals were used without further purification.

### 2.2. Preparation of Octadecane:Silicone (Oct/Si) composites

The compositions of pure silicone and Oct/Si composites are as shown in Table 1. Pure silicone rubber was prepared by mixing PlatSil® 73-20 Part A and PlatSil® 73-20 Part B in the same mass ratio. For the preparation of Oct/Si composites, as the silicone rubber mixture has a pour time of 5 min upon mixing of the two different components, Part B was mixed homogeneously with octadecane prior to mixing with Part A. Melted octadecane was added to Part B at 40 °C with constant stirring at 500 rpm using an overhead mechanical stirrer. To the homogenous mixture, Part A was then added and the mixture was allowed to stir for a further 2 min until homogenous. Thereafter, the composite mixture was casted onto a mold and cured at 35 °C for 4 h, followed by at room temperature for another 24 h.

### 2.3. Characterizations

#### 2.3.1. Chemical and structural analysis

Crystallinity of Octadecane, Silicone and Oct/Si composites were characterized by X-ray diffraction (XRD) using an automatic powder diffractometer (D8 Discover XRD, Bruker, USA) with Cu-K$\alpha$ radiation at a voltage of 50 kV and current of 0.8 mA. Samples were scanned at a rate of 16° $min^{-1}$ in the 2$\theta$ range of 10–60°. Structural analysis of the Oct/Si composites and silicone was studied by attenuated total reflection Fourier transform infrared (ATR-FTIR) spectroscopy and octadecane was analyzed by FTIR transmission mode (Spectrum 2000, PerkinElmer, USA), and the spectra were

**Table 1**
Composition of octadecane and silicone for the respective sample composites.

| Sample | Octadecane/Silicone (mass ratio) | Octadecane (g) ($M_{Oct}$) | PlatSil® 73-20 Part A (g) | PlatSil® 73-20 Part B (g) |
|---|---|---|---|---|
| **Si** | 0/1 | 0 | 4 | 4 |
| **50Oct-Si** | 5/5 | 4 | 2 | 2 |
| **60Oct-Si** | 6/4 | 4.8 | 1.6 | 1.6 |
| **70Oct-Si** | 7/3 | 5.6 | 1.2 | 1.2 |
| **80Oct-Si** | 8/2 | 6.4 | 0.8 | 0.8 |

recorded between a frequency range of 4000 to 600 $cm^{-1}$ with a resolution of 4 $cm^{-1}$ and a total of 16 scans.

#### 2.3.2. Form stability and leakage test

Oct/Si composites were subjected to a leakage test to determine the form stability as a form-stable PCM composite. Each sample was casted into a circular shape, and the respective initial mass, $M_0$ was measured using an analytical balance. The composites were placed on a filter paper in a petri dish, at a temperature of 40 °C in an oven. The mass of each composite, $M_n$, was measured at an interval of 1 h for over n hours. For each interval, the composites were taken out from the oven and gently dapped dry on the surface to remove residual leaked octadecane prior to weighing. The filter paper on the petri dish was then replaced, and the composites were placed back into the oven to continue the leakage test. The leakage test was conducted for 10 h. The leakage rate of octadecane can be calculated as

$$L = (M_0 - M_n) / M_0 \times 100\ \% \quad \text{Eq (1)}$$

and the percentage of octadecane loading during the leakage test can be calculated as

$$\text{Octadecane Loading} = (M_n - Si_T) / M_n \times 100\ \% \quad \text{Eq (2)}$$

where $Si_T$ is the total mass of Silicone (Part A and B) added for each sample.

### 2.4. Thermal analysis

The thermal stability of the Oct/Si composites was investigated using the thermal gravimetric analyzer (Q500, TA Instruments, USA) under a nitrogen gas flow rate of 60 mL/min. Samples were weighted between 8 mg and 12 mg into an alumina crucible, and heated from room temperature to 900 °C at a heating rate of 20 °C/min. The phase transition properties were investigated via the differential scanning calorimeter (Q100, TA Instruments, USA) under nitrogen gas with a flow rate of 50 mL/min. Samples were weighed between 3 mg and 7 mg and sealed in aluminum hermetic pans, and tested between a temperature range of −20 °C–70 °C at a heating rate of 10 °C/min.

### 2.5. Mechanical test

The tensile performance of the Oct/Si composites was tested using Instron 5569 Table Universal testing machine with a 100 N load cell capacity at a crosshead speed of 50 mm/min and a gauge length of 50 mm. The composites were cut into a rectangular stripe with dimensions of 110 mm × 10 mm with a thickness of approximately 3 mm. A total of five samples were prepared and tested for each composite. Tensile modulus, tensile strength, percentage elongation, and tensile toughness were determined along with the standard deviation.

## 3. Results and discussion

### 3.1. Chemical and structural analysis of PCMs

The crystallinity behavior of octadecane, silicone and Oct/Si composites was analyzed by X-ray diffraction (XRD) (Fig. S1). Silicone displayed a flat signal, indicating an amorphous structure. Octadecane showed clear indication of a crystalline structure with two crystal phases [56] where peaks at $2\theta = 11.38, 15.32, 39.54$ and $44.48°$ correspond to the (003), (004), (0−22) and (117) planes of the α-crystal, and peaks at $2\theta = 19.24, 19.74, 23.28$ and $34.92°$ are assigned to the (010), (011), (102) and (009) planes of the β-crystal form respectively [57,58]. The presence of α and β forms is due to the heterogeneous and homogeneous nucleation when in the melt state respectively [58]. Octadecane's main crystalline peaks were observed in all the Oct/Si composites, confirming its presence and composition in the respective composites.

ATR-FTIR and FTIR spectra of Oct/Si composites were measured and are given in Fig. S2. The characteristic stretching vibration of Si−*O*−Si backbone of silicone at 1007 $cm^{-1}$ was observed, while the peak at 785 $cm^{-1}$ is due to coupling of $-CH_3$ rocking and Si−C stretching vibrations [59–61]. FTIR spectrum of octadecane displayed peaks at 2917 $cm^{-1}$ and 2849 $cm^{-1}$ corresponding to the stretching of C−H bonds. Peaks at 1471 $cm^{-1}$ and 1369 $cm^{-1}$ correspond to C−H bending, and peak at 717 $cm^{-1}$ is due to in-plane rocking of $-CH_2-$ groups [57]. The spectrums of the Oct/Si composites shows a combination of the characteristic silicone and octadecane peaks with no new peaks formed. The trend of increased intensity of octadecane peaks for samples 50Oct-Si to 80 Oct-Si was also in good agreement with the increase in octadecane loading, suggesting that the two components were physically mixed well.

### 3.2. Form-stability

The composite samples were prepared as described in Section 2.2 and were poured into a circular mold for curing. The composites were subject to a leakage test as described in Section 2.3.1 to investigate its form stability as a PCM composite and the optimum octadecane loading capacities, and the results are summarized in Fig. 1. It was observed from Fig. 1A and B that a higher loading of octadecane led to a larger mass loss and thus percentage leakage, and this could be attributed to having lesser silicone as the matrix to interact with octadecane and encapsulate or bind them into the composite. 80Oct-Si resulted in the highest overall leakage of 68.53%, while 50Oct-Si gave the lowest leakage of 2.44%. This makes lower octadcane loading composites more favourable for the containment and encapsulation of the octadecane PCM material. Though higher octadecane loading samples led to higher percentage leakage, the final octadecane loading for 50Oct-Si to 70Oct-Si after 10 h was observed to hover between a narrow range of 43−48% as in Fig. 1C. This is especially so for 50Oct-Si and 60-Oct-Si, where the percentage leakage (Fig. 1B) and percentage octadecane remaining in each composite (Fig. 1C) seem to taper off close to

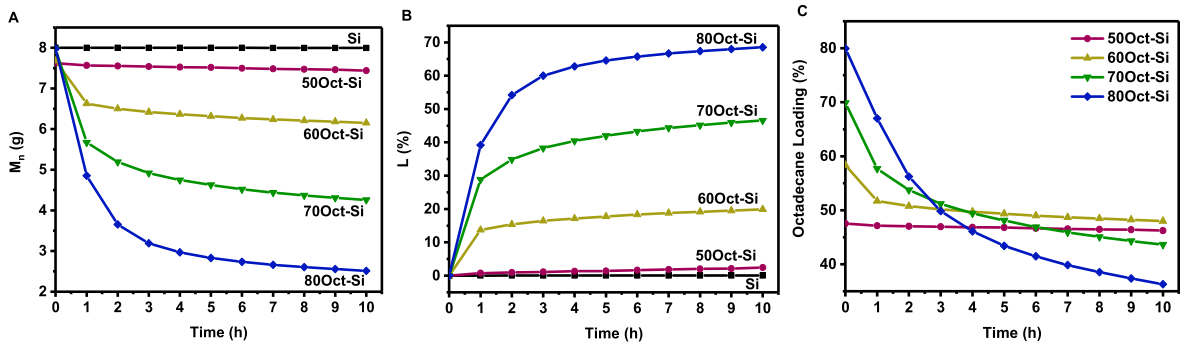


**Fig. 1.** A) Graph of mass of composite at nth hour time interval against time. B) Graph of leakage rate of octadecane against time. C) Graph of percentage of octadecane loading during the leakage test against time.

linearity with time. This suggests a favourable interaction between octadecane and silicone matrix at optimum loading capacity, helping to maintain a form-stable composite that retains at least 45% of PCM. 70Oct-Si appeared to be subjected to further minor loss of octadecane with time, while 80Oct-Si had a significant loss of octadecane with only 36.28% remaining at the end of the 10 h leakage test. These two higher loading composites has lesser silicone to interact with octadecane, leading to poorer performance in retaining the PCM.

With more octadecane leaked from higher loading composites, as observed in Fig. 2, there is no change in Silicone sample composite, 50Oct-Si and 60Oct-Si composites appears relatively unchanged with slight decrease in sample diameter and thickness, while 70Oct-Si and 80Oct-Si has significant shrinkage and deformities on the surface after the leakage test. From Fig. 3, silicone a natural elastomer exhibits great flexibility, where bending with the fingers allows it to conform to any desired shape without breaking. Both 50Oct-Si and 60Oct-Si also showed signs of flexibility before and after the leakage test, where it could be bent easily without breaking. This supports silicone as a suitable matrix for form-

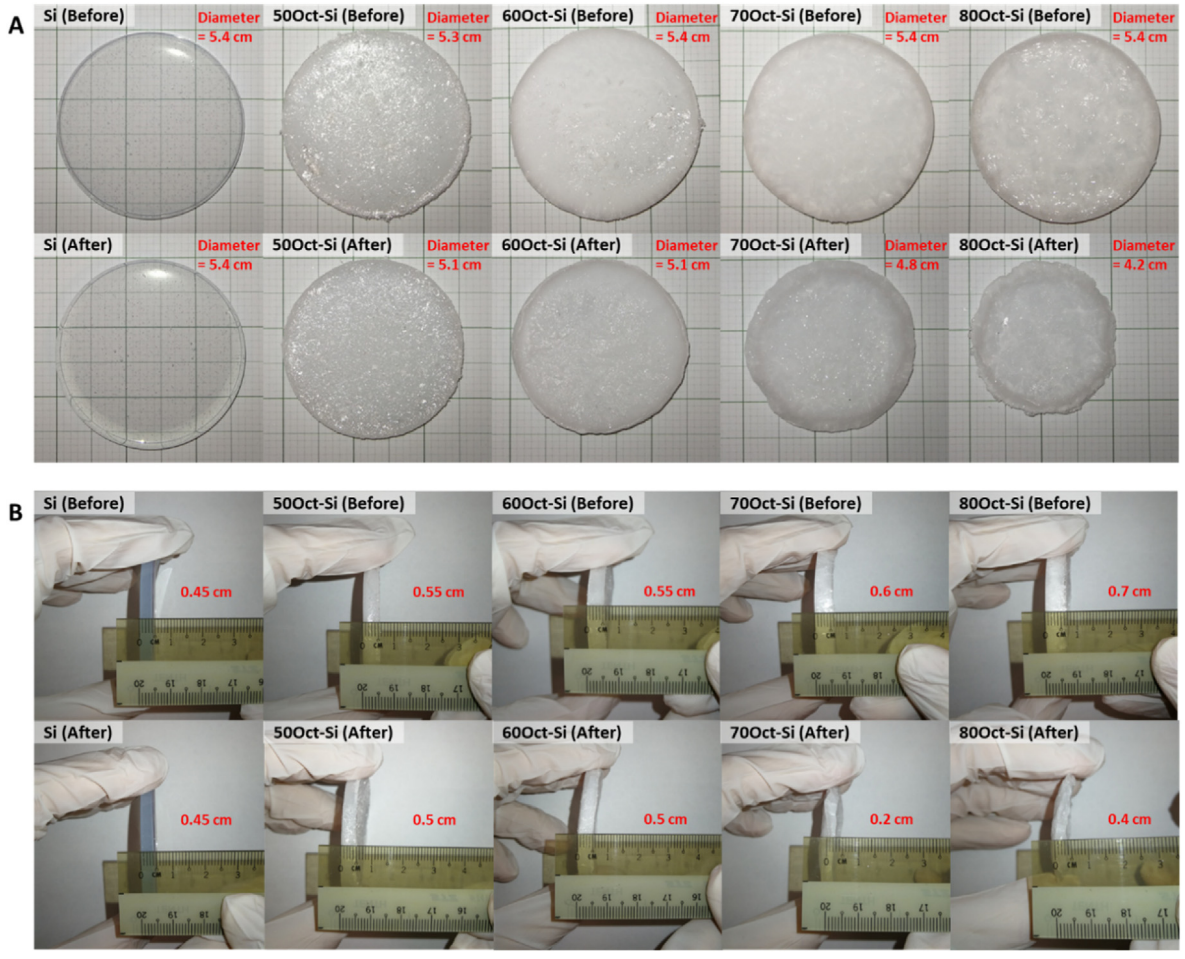


**Fig. 2.** Octadecane-Silicone Composites before and after subjected to leakage test from A) front view and B) side view.

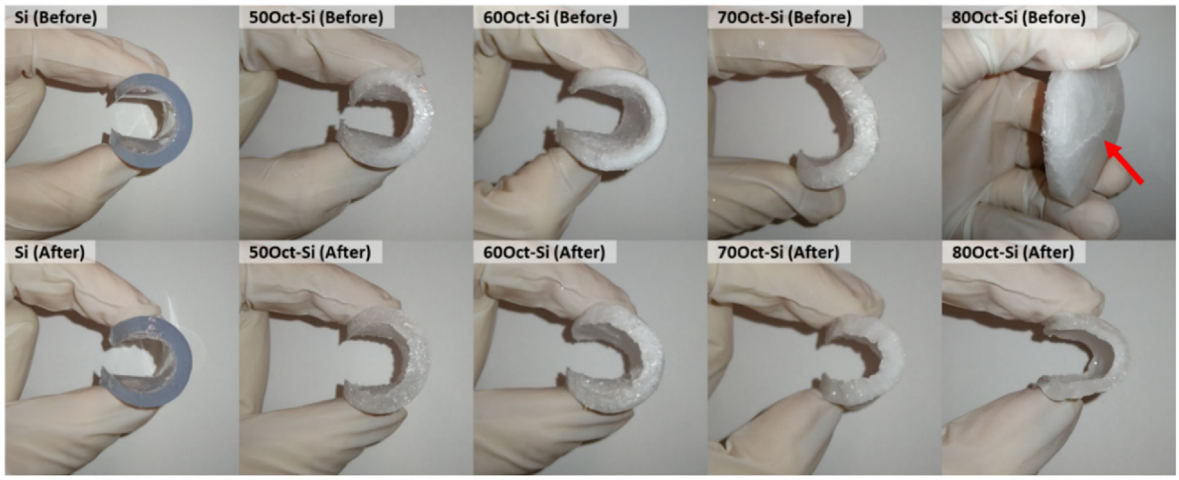


**Fig. 3.** Physical bending test for flexibility of composites. Red arrow points to crack observed.

stabilised octadecane-silicone composites. Tensile tests of these composites have been performed and results will be discussed in Section 3.3. As for 70Oct-Si and 80Oct-Si, the initial composites were rather stiff due to high loading of octadecane which dominates the characteristics of the composite, giving rise to a rather crystalline structure. Slight bending showed signs of crack, and this was especially evident in 80Oct-Si (indicated with a red arrow in Fig. 3). This rigid character was reduced after a significant amount of octadecane was leached out from the leakage test, and the composites consequently became more flexible but with a reduced thermal storage capacity.

### 3.3. Phase change properties and thermal stability

DSC analysis of the Oct/Si composites before and after the leakage test was performed, and the results are summarized in Fig. 4 and Table 2. From Fig. 4, octadecane was observed to give a single peak melting temperature ($T_m$) at 30.33 °C with an enthalpy

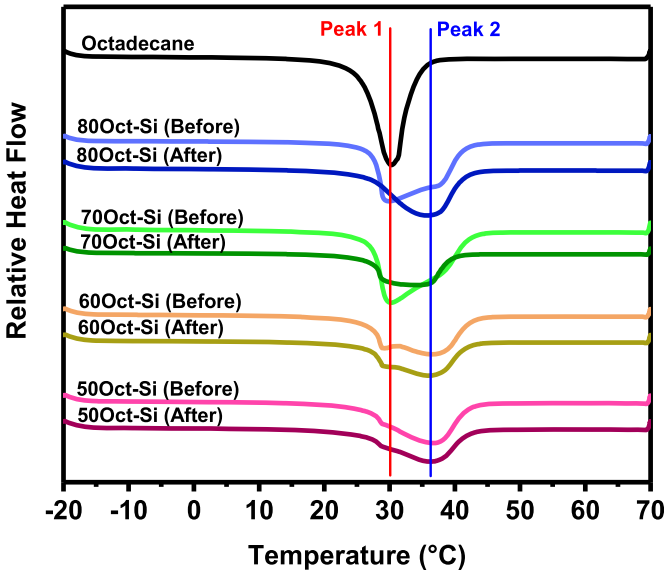


**Fig. 4.** DSC curves for Oct/Si PCM composites before and after the leakage test respectively.

of 215.6 J/g. However, two melting peaks were observed for the melting process of the Oct/Si composites with Peak 1 at a lower peak $T_m$ corresponding to the melting of bulk octadecane, and Peak 2 at a higher peak $T_m$ between 34.4 and 37.8 °C. Since silicone is an insulator, this shift to a higher $T_m$ could be due to a thermal insulation barrier formed by the silicone matrix, requiring a larger amount of energy to penetrate the matrix and melt the core octadecane [62]. Therefore, as the loading of octadecane decreased and consequently insulative silicone matrix content increased, Peak 1 is gradually suppressed while Peak 2 is enhanced. Another plausible possibility is due to the formation of metaphase for microencapsulated octadcane by silicone matrix. The microencapsulated octadecane is first encapsulated into a new metastable rotator phase from isotropic liquid rather than directly into the triclinic phase, as is the case for pure octadecane [63]. This observation is indeed indicative of successful trapping of octadecane in the silicone matrix, forming a form-stable PCM with low leakage [62]. Similarly with a portion of octadecane leaked out from the composites to almost similar levels between 35 and 50% (Fig. 1C) after the test, Peak 2 is enhanced with similar DSC profiles within the series. The composites with higher percentage leakage showed a more drastic change in the before and after DSC curves.

The latent heat can be estimated from the integration of the area under the peaks of the DSC heating curves, and the respective latent heat of each composite is summarized in Table 2. The latent heat of a PCM is directly proportionate to its composition within the mixture. Therefore, the latent heat of octadecane in the Oct/Si composite can be calculated based on the following equation:

$$\Delta H_O = \Delta H_{Oct} \cdot mo$$

where $\Delta H_{Oct}$ is the latent heat of octadecane, and $m_O$ is the mass fraction of octadecane within the composite. This is in line with the DSC results in Table 2, where the latent heat increased with the percentage loading of octadecane, and decreased after the leakage test to almost similar values.

TGA was performed for the Oct/Si composites to investigate its thermal stability, and the respective curves are shown in Fig. 5. Octadecane degraded almost completely through a one-step process, which started at about 90 °C and completed at around 230 °C. On the other hand, silicone was observed to be degraded via a three-step process, where the first degradation appeared to start from about 100 °C and ended at about 470 °C due to volatilization of

**Table 2**
DSC results of Octadecane/Silicone composites before and after the leakage test.

| Sample | | Latent Heat (J/g) | $T_m$ (Peak 1) (°C) | $T_m$ (Peak 2) (°C) | $T_{onset}$ (°C) |
|---|---|---|---|---|---|
| Octadecane | | 215.6 | 30.33 | NA | 25.71 |
| 50Oct-Si | Before | 103.8 | 28.85 | 36.71 | 26.90 |
| | After | 82.95 | 27.25 | 36.26 | 26.21 |
| 60Oct-Si | Before | 117.9 | 28.84 | 36.38 | 27.24 |
| | After | 105.7 | 28.97 | 35.97 | 27.28 |
| 70Oct-Si | Before | 149.2 | 30.30 | 37.17 | 27.49 |
| | After | 107.8 | – | 34.37 | 27.53 |
| 80Oct-Si | Before | 172.8 | 29.90 | 37.80 | 27.63 |
| | After | 108.7 | – | 35.76 | 26.53 |

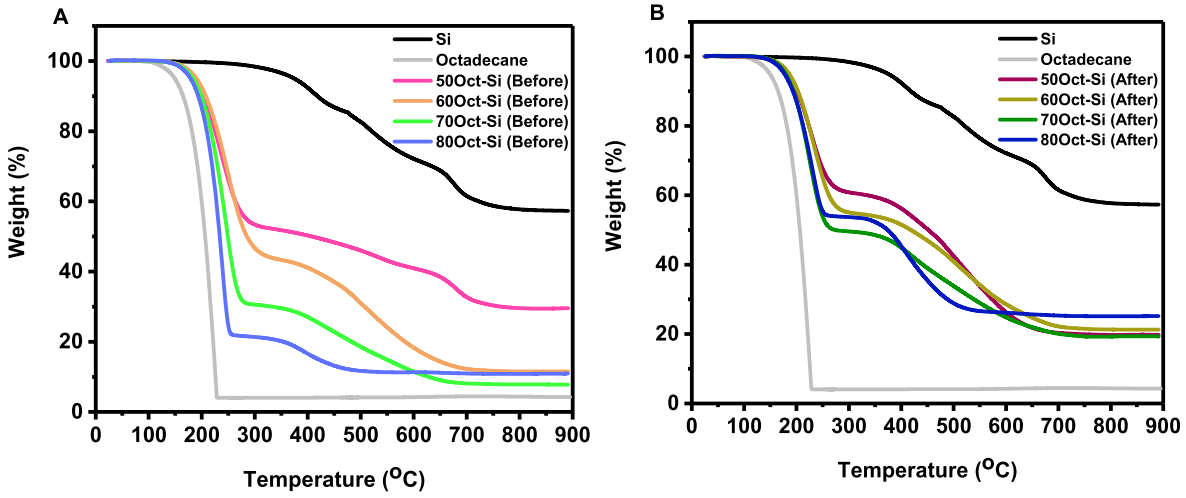


**Fig. 5.** A) TGA curves of Silicone, Octadecane and Oct/Si composites before leakage test. B) TGA curves of Silicone, Octadecane and Oct/Si composites after leakage test.

water and degradation from unzipping of terminal Si–OH groups [64–66]. The second degradation step commenced immediately and ended at about 620 °C, due to degradation and breakage of the main silicone polymer chain [67,68]. The last degradation step, which ended at around 800 °C was due to the conversion of silicone to silica [65,67,68], leaving behind a residue of 57.55 wt%. The composites before and after the leakage test showed a clear two-step degradation, where the first step generally starting at around 90–100 °C was attributed to the degradation of octadecane, and the percentage mass loss for each curve was in line with the amount of octadecane present in the respective composite. The second step was due to silicone degradation, and it commenced almost immediately after the first step. These DSC and TGA results indicate that the Oct/Si composites have been successfully prepared and possess good phase change properties and thermal stability during a temperature range of between 25 °C to 45 °C. It is also noteworthy that with the interaction between octadecane and silicone, the peak melting temperature is shifted from octadecane's melting temperature of 30.33 °C to the human body temperature range of 34.4–37.8 °C. This makes the composite more suitable for applications involving human body contact such as body temperature regulation and cooling, electronic wearable devices, human body waste heat harvesting and other potential applications.

### 3.4. Flexibility and durability

The Oct/Si composite samples were subject to mechanical testing to determine its flexibility and durability for applications such as wearable devices. As seen in Fig. 3, 70Oct-Si and 80Oct-Si composites started to crack upon light bending via the fingers, and thus these samples were deem unsuitable for mechanical tests. The Young's modulus, tensile strength, elongation at break and toughness were measured and calculated for the other three remaining samples, and the results are as given in Fig. 6. Silicone is a known elastomer [69] which has a low Young's modulus and a large elongation at break. The silicone used in this experiment was Platsil 73, and the technical data provided for this product was a tensile strength of 230 psi (equivalent to 1585.8 kPa) and an elongation of 460%. This is fairly consistent with the experimental data obtained for Si, where the tensile strength was 1497.07 kPa and elongation at break was 447.63%. It is clearly evident that pure silicone has high flexibility given its low Young's modulus of 235.41 kPa and a high toughness of 2685.64 kJ/m$^3$. As octadecane replaced half the amount of silicone in the composite (50Oct-Si), flexibility is slightly reduced where Young's modulus increased to 388.92 kPa, but the tensile strength of the composite dropped drastically to 386.89 kPa. This is possibly due to presence of octadecane within the silicone matrix, which disrupts the smooth polymeric network linkage throughout silicone. Consequently, the elongation at break drops to 341.42% and toughness is reduced by more than 3.5 times to 776.47 kJ/m$^3$. Increasing the octadecane concentration to 60% (60Oct-Si) reduced its flexibility by about 3.5 times, with Young's modulus jumping to 814.88 kPa, and tensile strength, elongation at break and toughness dropping to 224.15 kPa, 246.18% and 396.0 kJ/m$^3$ respectively. Despite the drastic decrease in Young's modulus when octadecane loading is more than half its composition, the two Oct/Si composites still exhibit great flexibility, just less durable compared to silicone itself. Hence, a form-stable PCM composite made of Oct/Si with 50% or 60% octadecane loading is still useful in various applications that require mild flexibility or conforming to

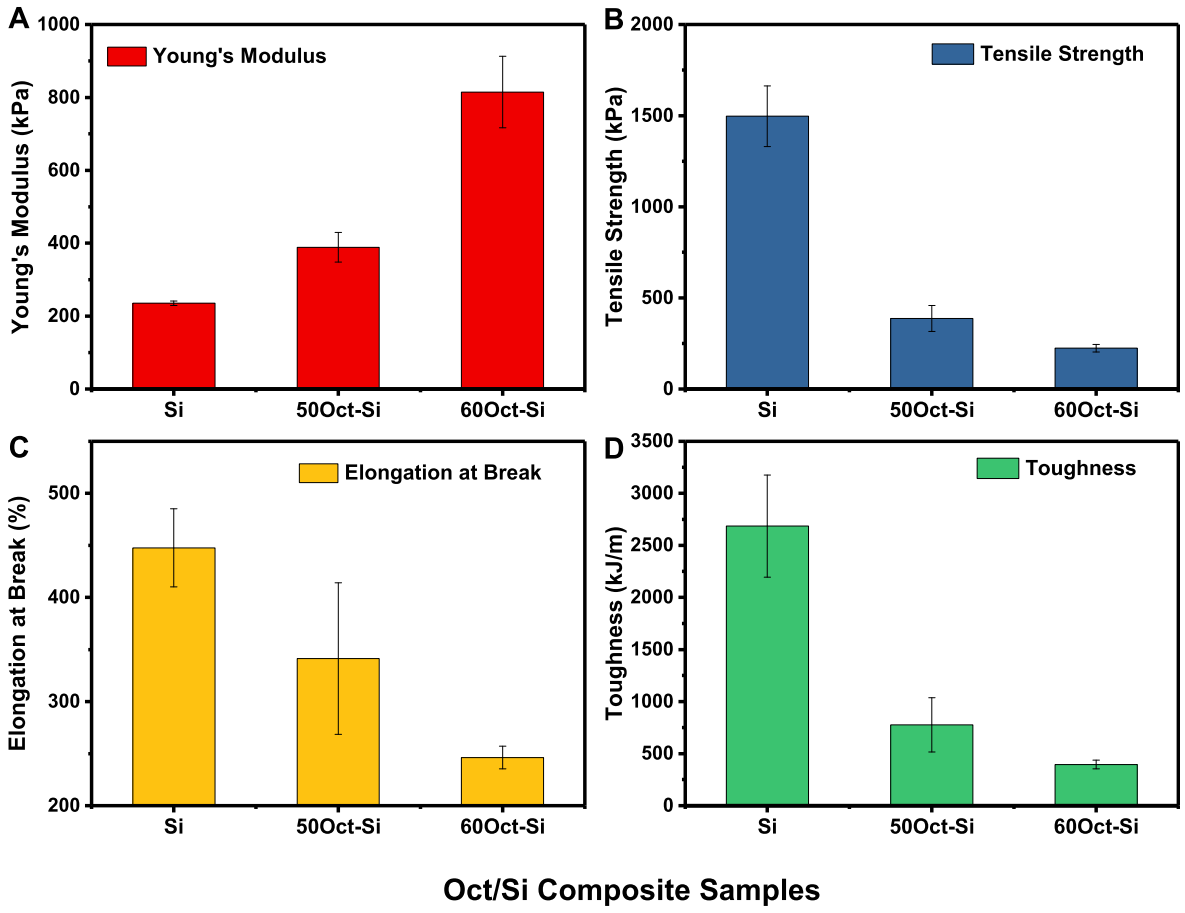


**Fig. 6.** Mechanical testing of properties for A) Young's modulus, B) tensile strength, C) elongation at break and D) toughness.

irregular shapes. We demonstrated a good example by using Oct/Si composites for flexible heat absorption and storage pads (More details are given in the Supporting Information).

## 4. Conclusion

PCMs have been widely used for thermal management applications; however, the leakage issue during phase change and its structural rigidity has hindered its wide applicability in industry. In this paper, a novel flexible form-stable PCM composite was successfully prepared by using silicone to encapsulate octadecane. Leakage tests showed minimal leakage for 50% octadecane loading samples (50Oct-Si) at 2.44%, and the composites eventually retained about 46–48% of the PCM. The DSC results indicated a shift in the melting peak of octadecane from 30.3 °C to a temperature between 34.4 and 37.8 °C, possible due to thermal insulation or microencapsulation by the silicone matrix. TGA data further confirmed its good thermal stability within this temperature range. Since the octadecane loading eventually stabilizes at around 46–48%, an initial loading of 50% octadecane for preparing the form-stabilised PCM would suffice, giving a significantly large latent heat of 103.8 J/g. The mechanical testing results exhibited that a 50% loading composite was flexible and durable, with Young's modulus of 388.92 kPa and elongation of 341.42%. Nevertheless, the tensile strength and toughness did fall short at 386.89 kPa and 776.47 kJ/m$^3$, but still acceptable for applications requiring mild flexibility. 50Oct/Si composite was also further fabricated into a heat absorption pad for energy storage application, showcasing the ability to absorb the waste heat from circular pipes.

In conclusion, an octadecane/silicone based form-stable PCM was successfully prepared, and 50% octadecane loading in its silicone matrix provides low leakage, good form stability, acceptable latent heat, good thermal stability, flexibility and durability for a wide range of applications requiring conformity to irregularities. This would open up a new direction for flexible form-stable PCMs with great potential for thermal management and energy. In our future works, we will be looking to integrate this flexible form-stable PCM composite with TE modules, electronics, wearable devices, and body temperature regulators for effective energy harvesting and management.

## Credit author statement

Xiang Yun Debbie Soo – Conceptualization, Methodology, Investigation, Writing – original draft, Zhuang Mao Png – Methodology, Writing – review & editing, Ming Hui Chua – Validation, Writing – review & editing, Jayven Chee Chuan Yeo – Investigation, Writing – review & editing,Pin Jin Ong – Investigation, Suxi Wang – Investigation, Xizu Wang – Resources, Ady Suwardi – Resources, Alex Qingyu Yan – Writing – review & editing, Supervision, Xian Jun Loh – Writing – review & editing, Supervision, Jianwei Xu – Writing – review & editing, Supervision, Qiang Zhu – Conceptualization, Supervision, Funding acquisition, Writing – review & editing.

## Declaration of competing interest

The authors declare that they have no known competing

financial interests or personal relationships that could have appeared to influence the work reported in this paper.

## Acknowledgment and Funding Source

The authors acknowledge the financial support from the Agency for Science, Technology and Research (A*STAR), Science and Engineering Research Council, and A*ccelerate Technologies for this work (Grant No.: GAP/2019/00314).

## Appendix A. Supplementary data

Supplementary data to this article can be found online at https://doi.org/10.1016/j.mtadv.2022.100227.

## References

[1] R. Baetens, B.P. Jelle, A. Gustavsen, Aerogel insulation for building applications: a state-of-the-art review, Energy Build. 43 (2011) 761–769, https://doi.org/10.1016/j.enbuild.2010.12.012.
[2] M. Ashouri, F.R. Astaraei, R. Ghasempour, M.H. Ahmadi, M. Feidt, Optimum insulation thickness determination of a building wall using exergetic life cycle assessment, Appl. Therm. Eng. 106 (2016) 307–315, https://doi.org/10.1016/j.applthermaleng.2016.05.190.
[3] Á. Lakatos, F. Kalmár, Investigation of thickness and density dependence of thermal conductivity of expanded polystyrene insulation materials, Mater. Struct. 46 (2013) 1101–1105, https://doi.org/10.1617/s11527-012-9956-5.
[4] K.L. Uemoto, N.M. Sato, V.M. John, Estimating thermal performance of cool colored paints, Energy Build. 42 (2010) 17–22, https://doi.org/10.1016/j.enbuild.2009.07.026.
[5] P. Meenakshi, M. Selvaraj, Bismuth titanate as an infrared reflective pigment for cool roof coating, Sol. Energy Mater. Sol. Cell. 174 (2018) 530–537, https://doi.org/10.1016/j.solmat.2017.09.048.
[6] T. Thongkanluang, P. Limsuwan, P. Rakkwamsuk, Preparation and application of high near-infrared reflective green pigment for ceramic tile roofs, Int. J. Appl. Ceram. Technol. 8 (2011) 1451–1458, https://doi.org/10.1111/j.1744-7402.2010.02599.x.
[7] M.H. Elsheikh, D.A. Shnawah, M.F.M. Sabri, S.B.M. Said, M.H. Hassan, M.B.A. Bashir, M. Mohamad, A review on thermoelectric renewable energy: principle parameters that affect their performance, Renew. Sustain. Energy Rev. 30 (2014) 337–355, https://doi.org/10.1016/j.rser.2013.10.027.
[8] Q. Zhu, E. Yildirim, X. Wang, X.Y.D. Soo, Y. Zheng, T.L. Tan, G. Wu, S.-W. Yang, J. Xu, Improved alignment of pedot: pss induced by in-situ crystallization of "green" dimethylsulfone molecules to enhance the polymer thermoelectric performance, Front. Chem. 7 (2019) 783, https://doi.org/10.3389/fchem.2019.00783.
[9] D. Zhao, G. Tan, A review of thermoelectric cooling: materials, modeling and applications, Appl. Therm. Eng. 66 (2014) 15–24, https://doi.org/10.1016/j.applthermaleng.2014.01.074.
[10] Q. Zhu, E. Yildirim, X. Wang, A.K.K. Kyaw, T. Tang, X.Y.D. Soo, Z.M. Wong, G. Wu, S.-W. Yang, J. Xu, Effect of substituents in sulfoxides on the enhancement of thermoelectric properties of pedot: pss: Experimental and modelling evidence, Mol. Syst. Design Eng. 5 (2020) 976–984, https://doi.org/10.1039/D0ME00032A.
[11] T.A. Yemata, A.K.K. Kyaw, Y. Zheng, X. Wang, Q. Zhu, W.S. Chin, J. Xu, Enhanced thermoelectric performance of poly (3, 4-ethylenedioxythiophene): poly (4-styrenesulfonate)(pedot: pss) with long-term humidity stability via sequential treatment with trifluoroacetic acid, Polym. Int. 69 (2020) 84–92, https://doi.org/10.1002/pi.5921.
[12] Q. Zhu, S. Wang, X. Wang, A. Suwardi, M.H. Chua, X.Y.D. Soo, J. Xu, Bottom-up engineering strategies for high-performance thermoelectric materials, Nano-Micro Lett. 13 (2021) 1–38, https://doi.org/10.1007/s40820-021-00637-z.
[13] L.F. Cabeza, A. Castell, C.d. Barreneche, A. De Gracia, A. Fernández, Materials used as pcm in thermal energy storage in buildings: a review, Renew. Sustain. Energy Rev. 15 (2011) 1675–1695, https://doi.org/10.1016/j.rser.2010.11.018.
[14] A.F. Regin, S. Solanki, J. Saini, Heat transfer characteristics of thermal energy storage system using pcm capsules: a review, Renew. Sustain. Energy Rev. 12 (2008) 2438–2458, https://doi.org/10.1016/j.rser.2007.06.009.
[15] P.J. Ong, Z.M. Png, X.Y.D. Soo, X. Wang, A. Suwardi, M.H. Chua, Q. Zhu, J.W. Xu, Surface modification of microencapsulated phase change materials with nanostructures for enhancement of their thermal conductivity, Mater. Chem. Phys. (2021) 125438, https://doi.org/10.1016/j.matchemphys.2021.125438.
[16] Z.M. Png, X.Y.D. Soo, M.H. Chua, P.J. Ong, A. Suwardi, C.K.I. Tan, J. Xu, Q. Zhu, Strategies to reduce the flammability of organic phase change materials: a review, Sol. Energy 231 (2022) 115–128, https://doi.org/10.1016/j.solener.2021.11.057.
[17] Z.M. Png, X.Y.D. Soo, M.H. Chua, P.J. Ong, J. Xu, Q. Zhu, Triazine derivatives as organic phase change materials with inherently low flammability, J. Mater. Chem. (2022), https://doi.org/10.1039/D1TA07422A.
[18] A. Safari, R. Saidur, F. Sulaiman, Y. Xu, J. Dong, A review on supercooling of phase change materials in thermal energy storage systems, Renew. Sustain. Energy Rev. 70 (2017) 905–919, https://doi.org/10.1016/j.rser.2016.11.272.
[19] P.K.S. Rathore, S.K. Shukla, Potential of macroencapsulated pcm for thermal energy storage in buildings: a comprehensive review, Construct. Build. Mater. 225 (2019) 723–744, https://doi.org/10.1016/j.conbuildmat.2019.07.221.
[20] L.F. Cabeza, C. Castellon, M. Nogues, M. Medrano, R. Leppers, O. Zubillaga, Use of microencapsulated pcm in concrete walls for energy savings, Energy Build. 39 (2007) 113–119, https://doi.org/10.1016/j.enbuild.2006.03.030.
[21] C. Liu, Z. Rao, J. Zhao, Y. Huo, Y. Li, Review on nanoencapsulated phase change materials: preparation, characterization and heat transfer enhancement, Nano Energy 13 (2015) 814–826, https://doi.org/10.1016/j.nanoen.2015.02.016.
[22] Y. Konuklu, M. Ostry, H.O. Paksoy, P. Charvat, Review on using microencapsulated phase change materials (pcm) in building applications, Energy Build. 106 (2015) 134–155, https://doi.org/10.1016/j.enbuild.2015.07.019.
[23] R. Wen, Z. Huang, Y. Huang, X. Zhang, X. Min, M. Fang, Y.g. Liu, X. Wu, Synthesis and characterization of lauric acid/expanded vermiculite as form-stabilized thermal energy storage materials, Energy Build. 116 (2016) 677–683, https://doi.org/10.1016/j.enbuild.2016.01.023.
[24] A. Sarı, A. Karaipekli, Preparation, thermal properties and thermal reliability of capric acid/expanded perlite composite for thermal energy storage, Mater. Chem. Phys. 109 (2008) 459–464, https://doi.org/10.1016/j.matchemphys.2007.12.016.
[25] H. Yi, W. Zhan, Y. Zhao, S. Qu, W. Wang, P. Chen, S. Song, A novel core-shell structural montmorillonite nanosheets/stearic acid composite pcm for great promotion of thermal energy storage properties, Sol. Energy Mater. Sol. Cell. 192 (2019) 57–64, https://doi.org/10.1016/j.solmat.2018.12.015.
[26] S. Karaman, A. Karaipekli, A. Sarı, A. Bicer, Polyethylene glycol (peg)/diatomite composite as a novel form-stable phase change material for thermal energy storage, Sol. Energy Mater. Sol. Cell. 95 (2011) 1647–1653, https://doi.org/10.1016/j.solmat.2011.01.022.
[27] H. Yu, J. Gao, Y. Chen, Y. Zhao, Preparation and properties of stearic acid/expanded graphite composite phase change material for low-temperature solar thermal application, J. Therm. Anal. Calorim. 124 (2016) 87–92, https://doi.org/10.1007/s10973-015-5151-6.
[28] P.M. Gilart, Á.Y. Martínez, M.G. Barriuso, C.M. Martínez, Development of pcm/carbon-based composite materials, Sol. Energy Mater. Sol. Cell. 107 (2012) 205–211, https://doi.org/10.1016/j.solmat.2012.06.014.
[29] Y. Li, X. Huang, Y. Li, Z. Xi, G. Hai, Z. Tao, G. Wang, Shape-stabilized phase-change materials supported by eggplant-derived porous carbon for efficient solar-to-thermal energy conversion and storage, Sustain. Energy Fuels 4 (2020) 1764–1772, https://doi.org/10.1039/C9SE01272A.
[30] T. Nomura, C. Zhu, N. Sheng, K. Tabuchi, A. Sagara, T. Akiyama, Shape-stabilized phase change composite by impregnation of octadecane into mesoporous sio2, Sol. Energy Mater. Sol. Cell. 143 (2015) 424–429, https://doi.org/10.1016/j.solmat.2015.07.028.
[31] X. Kong, C. Yao, P. Jie, Y. Liu, C. Qi, X. Rong, Development and thermal performance of an expanded perlite-based phase change material wallboard for passive cooling in building, Energy Build. 152 (2017) 547–557, https://doi.org/10.1016/j.enbuild.2017.06.067.
[32] Y. Tang, D. Su, X. Huang, G. Alva, L. Liu, G. Fang, Synthesis and thermal properties of the ma/hdpe composites with nano-additives as form-stable pcm with improved thermal conductivity, Appl. Energy 180 (2016) 116–129, https://doi.org/10.1016/j.apenergy.2016.07.106.
[33] L. Li, G. Wang, C. Guo, Influence of intumescent flame retardant on thermal and flame retardancy of eutectic mixed paraffin/polypropylene form-stable phase change materials, Appl. Energy 162 (2016) 428–434, https://doi.org/10.1016/j.apenergy.2015.10.103.
[34] Y. Lv, X. Yang, X. Li, G. Zhang, Z. Wang, C. Yang, Experimental study on a novel battery thermal management technology based on low density polyethylene-enhanced composite phase change materials coupled with low fins, Appl. Energy 178 (2016) 376–382, https://doi.org/10.1016/j.apenergy.2016.06.058.
[35] P. Sobolciak, M. Karkri, M.A. Al-Maadeed, I. Krupa, Thermal characterization of phase change materials based on linear low-density polyethylene, paraffin wax and expanded graphite, Renew. Energy 88 (2016) 372–382, https://doi.org/10.1016/j.renene.2015.11.056.
[36] A. Trigui, M. Karkri, I. Krupa, Thermal conductivity and latent heat thermal energy storage properties of ldpe/wax as a shape-stabilized composite phase change material, Energy Convers. Manag. 77 (2014) 586–596, https://doi.org/10.1016/j.enconman.2013.09.034.
[37] F. Chen, M. Wolcott, Polyethylene/paraffin binary composites for phase change material energy storage in building: a morphology, thermal properties, and paraffin leakage study, Sol. Energy Mater. Sol. Cell. 137 (2015) 79–85, https://doi.org/10.1016/j.solmat.2015.01.010.
[38] M. Mu, P. Basheer, W. Sha, Y. Bai, T. McNally, Shape stabilised phase change materials based on a high melt viscosity hdpe and paraffin waxes, Appl. Energy 162 (2016) 68–82, https://doi.org/10.1016/j.apenergy.2015.10.030.
[39] K. Merlin, D. Delaunay, J. Soto, L. Traonvouez, Heat transfer enhancement in latent heat thermal storage systems: comparative study of different solutions and thermal contact investigation between the exchanger and the pcm, Appl. Energy 166 (2016) 107–116, https://doi.org/10.1016/j.apenergy.2016.01.012.
[40] W. Wu, W. Wu, S. Wang, Form-stable and thermally induced flexible composite phase change material for thermal energy storage and thermal management applications, Appl. Energy 236 (2019) 10–21, https://doi.org/10.1016/j.apenergy.2018.11.071.
[41] Q. Sun, H. Zhang, J. Xue, X. Yu, Y. Yuan, X. Cao, Flexible phase change materials

for thermal storage and temperature control, Chem. Eng. J. 353 (2018) 920–929, https://doi.org/10.1016/j.cej.2018.07.185.
[42] X. Lu, H. Yu, L. Zhang, Y. Zheng, L. Xu, Y. Zhao, Flexible ethylene propylene diene monomer/paraffin wax vulcanizate with simultaneously increased mechanical strength, thermal-energy storage, and shape-memory behavior, Energy Fuel. 34 (2020) 9020–9029, https://doi.org/10.1021/acs.energyfuels.0c01800.
[43] K. Yu, Y. Liu, F. Sun, M. Jia, Y. Yang, Graphene-modified hydrate salt/uv-curable resin form-stable phase change materials: continuously adjustable phase change temperature and ultrafast solar-to-thermal conversion, Energy Fuel. 33 (2019) 7634–7644, https://doi.org/10.1021/acs.energyfuels.9b01165.
[44] T. Wang, N. Wu, H. Li, Q.L. Lu, Y. Jiang, Preparation and properties of a form-stable phase-change hydrogel for thermal energy storage, J. Appl. Polym. Sci. 133 (2016), https://doi.org/10.1002/app.43836.
[45] J. Hirschey, K.R. Gluesenkamp, A. Mallow, S. Graham, Review of Inorganic Salt Hydrates with Phase Change Temperature in Range of 5 to 60° C and Material Cost Comparison with Common Waxes, 2018. https://docs.lib.purdue.edu/ihpbc/320/.
[46] J.F. Su, L.X. Wang, L. Ren, Z. Huang, X.W. Meng, Preparation and characterization of polyurethane microcapsules containing n-octadecane with styrene-maleic anhydride as a surfactant by interfacial polycondensation, J. Appl. Polym. Sci. 102 (2006) 4996–5006. https://doi-org.ejproxy.a-star.edu.sg/10.1002/app.25001.
[47] Z. Zhang, G. Shi, S. Wang, X. Fang, X. Liu, Thermal energy storage cement mortar containing n-octadecane/expanded graphite composite phase change material, Renew. Energy 50 (2013) 670–675, https://doi.org/10.1016/j.renene.2012.08.024.
[48] R. Zhao, J. Gu, J. Liu, Optimization of a phase change material based internal cooling system for cylindrical li-ion battery pack and a hybrid cooling design, Energy 135 (2017) 811–822, https://doi.org/10.1016/j.energy.2017.06.168.
[49] X. Wan, J. Fan, A new method for measuring the thermal regulatory properties of phase change material (pcm) fabrics, Meas. Sci. Technol. 20 (2009), 025110, https://doi.org/10.1088/0957-0233/20/2/025110.
[50] Y. Yang, W. Gao, Wearable and flexible electronics for continuous molecular monitoring, Chem. Soc. Rev. 48 (2019) 1465–1491. https://doi-org.ejproxy.a-star.edu.sg/10.1039/C7CS00730B.
[51] L. Namitha, M. Sebastian, High permittivity ceramics loaded silicone elastomer composites for flexible electronics applications, Ceram. Int. 43 (2017) 2994–3003, https://doi.org/10.1016/j.ceramint.2016.11.080.
[52] P. Mazurek, M.A. Brook, A.L. Skov, Glycerol–silicone elastomers as active matrices with controllable release profiles, Langmuir 34 (2018) 11559–11566, https://doi.org/10.1021/acs.langmuir.8b02039.
[53] Z. Fu, L. Su, J. Li, R. Yang, Z. Zhang, M. Liu, J. Li, B. Li, Elastic silicone encapsulation of n-hexadecyl bromide by microfluidic approach as novel microencapsulated phase change materials, Thermochim. Acta 590 (2014) 24–29, https://doi.org/10.1016/j.tca.2014.06.008.
[54] Y. Guo, W. Yang, Z. Jiang, F. He, K. Zhang, R. He, J. Wu, J. Fan, Silicone rubber/paraffin@ silicon dioxide form-stable phase change materials with thermal energy storage and enhanced mechanical property, Sol. Energy Mater. Sol. Cell. 196 (2019) 16–24, https://doi.org/10.1016/j.solmat.2019.03.034.
[55] Y. Zhang, W. Li, J. Huang, M. Cao, G. Du, Expanded graphite/paraffin/silicone rubber as high temperature form-stabilized phase change materials for thermal energy storage and thermal interface materials, Materials 13 (2020) 894, https://doi.org/10.3390/ma13040894.
[56] Y. Zhu, S. Liang, K. Chen, X. Gao, P. Chang, C. Tian, J. Wang, Y. Huang, Preparation and properties of nanoencapsulated n-octadecane phase change material with organosilica shell for thermal energy storage, Energy Convers. Manag. 105 (2015) 908–917, https://doi.org/10.1016/j.enconman.2015.08.048.
[57] G.T. Nguyen, H.S. Hwang, J. Lee, D.A. Cha, I. Park, N-octadecane/fumed silica phase change composite as building envelope for high energy efficiency, Nanomaterials 11 (2021) 566, https://doi.org/10.3390/nano11030566.
[58] L. Zhao, H. Wang, J. Luo, Y. Liu, G. Song, G. Tang, Fabrication and properties of microencapsulated n-octadecane with tio2 shell as thermal energy storage materials, Sol. Energy 127 (2016) 28–35, https://doi.org/10.1016/j.solener.2016.01.018.
[59] S.I. Salih, J.K. Oleiwi, H.M. Ali, Modification of silicone rubber by added pmma and natural nanoparticle used for maxillofacial prosthesis applications, ARPN J. Eng. Appl. Sci. 14 (2019). https://www.researchgate.net/profile/Jawad-Oleiwi/publication/331808493_Modification_of_silicone_rubber_by_added_PMMA_and_natural_nanoparticle_used_for_maxillofacial_prosthesis_applications/links/5c8cff0e92851c1df9447a34/Modification-of-silicone-rubber-by-added-PMMA-and-natural-nanoparticle-used-for-maxillofacial-prosthesis-applications.pdf.
[60] X. Wen, X. Yuan, L. Lan, L. Hao, Y. Wang, S. Li, H. Lu, Z. Bao, Rtv silicone rubber degradation induced by temperature cycling, Energies 10 (2017) 1054, https://doi.org/10.3390/en10071054.
[61] J. Feng, Q. Zhang, Z. Tu, W. Tu, Z. Wan, M. Pan, H. Zhang, Degradation of silicone rubbers with different hardness in various aqueous solutions, Polym. Degrad. Stabil. 109 (2014) 122–128, https://doi.org/10.1016/j.polymdegradstab.2014.07.011.
[62] M. Aludin, S.S. Akmal, Preparation and characterization of form-stable paraffin/polycaprolactone composites as phase change materials for thermal energy storage, MATEC Web Conf. 97 (2017), 01094, https://doi.org/10.1051/matecconf/20179701094.
[63] B. Xie, G. Liu, S. Jiang, Y. Zhao, D. Wang, Crystallization behaviors of n-octadecane in confined space: crossover of rotator phase from transient to metastable induced by surface freezing, J. Phys. Chem. B 112 (2008) 13310–13315, https://doi.org/10.1021/jp712160k.
[64] S.K. Choi, Photonanotechnology for Therapeutics and Imaging, Elsevier, 2020.
[65] W. Zhou, H. Yang, X. Guo, J. Lu, Thermal degradation behaviors of some branched and linear polysiloxanes, Polym. Degrad. Stabil. 91 (2006) 1471–1475, https://doi.org/10.1016/j.polymdegradstab.2005.10.005.
[66] Y. Liu, Y. Huang, L. Liu, Effects of trisilanolisobutyl-poss on thermal stability of methylsilicone resin, Polym. Degrad. Stabil. 91 (2006) 2731–2738, https://doi.org/10.1016/j.polymdegradstab.2006.04.031.
[67] R. Huang, J. Yao, Q. Mu, D. Peng, H. Zhao, Z. Yang, Study on the synthesis and thermal stability of silicone resin containing trifluorovinyl ether groups, Polymers 12 (2020) 2284, https://doi.org/10.3390/polym12102284.
[68] Z. Yang, S. Han, R. Zhang, S. Feng, C. Zhang, S. Zhang, Effects of silphenylene units on the thermal stability of silicone resins, Polym. Degrad. Stabil. 96 (2011) 2145–2151, https://doi.org/10.1016/j.polymdegradstab.2011.09.014.
[69] S.C. Shit, P. Shah, A review on silicone rubber, Natl. Acad. Sci. Lett. 36 (2013) 355–365, https://doi.org/10.1007/s40009-013-0150-2.